ELSEVIER

www.elsevier.nl/locate/jorganchem

Journal of Organometallic Chemistry 617–618 (2001) 364–375

Journal of Organometallic Chemistry

Helical mono and dinuclear mercury(II) *N*-heterocyclic carbene complexes

Kwang-Ming Lee, Jack C.C. Chen, Ivan J.B. Lin *

Department of Chemistry, Fu-Jen Catholic University, Hsinchuang, Taipei 24205, Taiwan, ROC

Received 20 July 2000

Abstract

A series of mono and dicationic carbene precursors have been synthesized. Reactions of these precursors with $Hg(OAc)_2$ produce helical mononuclear and dinuclear mercury(II) carbene complexes. Five structures, including two ligand precursors and three mercury(II) carbene complexes have been analyzed by single crystal X-ray diffraction. Several intermediates have been identified during the course of reaction. Based on these observed intermediates, three different reaction pathways have been proposed.

Keywords: Carbene complexes; Double helicates; Supramolecules; Mercury

1. Introduction

Metal complexes of carbenes based on imidazol-2-ylidene (imy) have received much attention in the past few years. A major reason is that these *N*-heterocyclic carbenes can stabilize both high as well as low oxidation metal ions and form stable carbene complexes with a wide range of metal ions [1–5]. Early in 1975 an analogy between imy carbene and phosphine had been proposed [6]. Many organic reactions using metal–carbene complexes as catalysts have thus been investigated [7–16]. However, the use of imy carbene to form helical complexes is very rare. Self-assembled supramolecular helicates are relevant to biological and material sciences. For instance, their similarity in the self-assembly process and topology to natural α-helical polypeptides and double-helical nucleic acids [17–19]. Therefore, it is important to design ligands that facilitate self-assembly and recognition in the formation of helical complexes. Many pioneering studies are based on nitrogen and oxygen donor ligands [20–22], but up to the present, no metal–carbene helical complex has been reported prior to our work.

We have reported the facile synthesis of carbene complexes of Ag^{I}, Au^{I} and Pd^{II}, and investigated their properties such as aggregation, luminescence and mesomorphism [23–26]. Among the increasing literatures of imidazol-2-ylidene carbene complexes, only few mercury carbene complexes have been reported [27–32]. One latest report of mercury carbene complex based on *N*-ferrocenyl-*N′*-methyl-benzimidazol-2-ylidene has been reported by Bildstein et al. Owing to its poor solubility, only IR and mass spectral data are available [32]. Recently, we reported the preliminary results of double helical mercury carbene complexes based on 2,6-bis(1-methylimidazol-2-ylidyl)pyridine, which has two carbenes linked by a pyridine [33]. In order to understand the chemistry of mercury carbene complexes more and to gain an insight into the formation of double helical mercury carbene complexes, we set out to synthesize a series of mononuclear (Scheme 1) and dinuclear (Scheme 2) mercury carbene complexes.

2. Results and discussion

Carbene ligand precursors, [MeHimy-pymd]Cl, **1**(Cl); [MeHimy-pymd][PF_6], **1**(PF_6); [py-Himy-py]Cl, **2**(Cl); [py-Himy-py][PF_6], **2**(PF_6); [MeHimy-py-imyHMe]Br_2, **5**(Br); [MeHimy-py-imyHMe][PF_6]$_2$, **5**(PF_6); [MeHimy-

* Corresponding author. Tel.: +886-2-29031111, ext. 3570; fax: +886-2-29023209.

E-mail address: chem1001@mails.fju.edu.tw (I.J.B. Lin).

0022-328X/01/$ - see front matter
PII: S0022-328X(00)00617-3

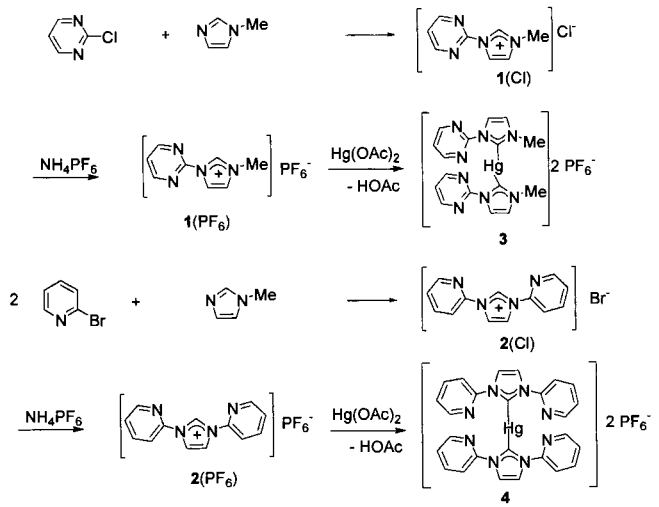

Scheme 1. Synthesis of the ligand precursors and mononuclear carbene complexes.

pydz-imyHMe]Cl_2, **6**(Cl); [MeHimy-pydz-imyHMe]$[PF_6]_2$, **6**(PF_6); [pymd-HimyC_3imyH-pymd]Br_2, **7**(Br) and [pymd-HimyC_3imyH-pymd]$[PF_6]_2$, **7**(PF_6); (py = pyridine, pydz = pyridazine, C_3 = propyl, pymd = pyrimidine), were synthesized by reacting the corresponding heterocyclic linkers with two molar ratios of 1-methylimidazole (Schemes 1 and 2). These precursors can be collectively grouped to **1**, **2**, **5**, **6** and **7**. Ligand precursors with chloride or bromide anions have very poor solubility in common organic solvents and are therefore difficult to use to prepare metal complexes. Ligand precursors with PF_6^- anions were obtained from their corresponding chloride or bromide salts by metathesis in water. These PF_6^- salts are soluble in acetonitrile and acetone and are used for the synthesis of metal–carbene complexes.

2.1. Mononuclear ligand precursors and mercury carbene complexes

The design of imidazolium salts of **1** and **2** are based on several reasons. First, the electron withdrawing property of pyrimidyl and pyridyl groups may facilitate the carbene formation. A second reason is that these pyrimidyl and pyridyl groups have lone pair electrons on the *N* atoms and also have slightly acidic ring C–H protons, such that formation of supramolecules is possible through extended H-bonds. Furthermore, pyrimidyl and pyridyl are themselves potential donor ligands, which together with the carbene donor site form interesting multidentate ligands suitable for the study of supramolecular complex chemistry. Ligand precursors **1**, which after deprotonating the 2-carbene hydrogens, have potentially one carbene carbon and one nitrogen binding sites, while precursors **2** have one carbene carbon and two nitrogen binding sites. Fig. 1 is the crystal structure of **1**(PF_6). All the bond angles and bond distances of imidazolium ring and methyl group are comparable to that reported for [MeimyHEt][PF_6] [34]. The pyrimidine ring tilts slightly from the imidazolium ring by an angle of 11.6°. The three protons (H2), (H42) and (H7) coming individually from the imidazolium ring, methyl group and pyrimidine act as hydrogen bonding donors. Hydrogen bonds formed by these hydrogen atoms and two F atoms of PF_6^- generate a hydrogen bonding sheet with H···F distances of 2.440, 2.473 and 2.523 Å, respectively. The adjacent sheets are stacked through π–π interactions of the pyrimidine rings. The acidity of the 2-carbene hydrogens of **1** and **2** is affected by the electron withdrawing ability of the pyrimidyl or pyridyl group. The ^{1}H-NMR spectrum of **1**(PF_6) and **2**(PF_6) shows that the chemical shifts of the H2 protons are 9.45 and 10.06 ppm,

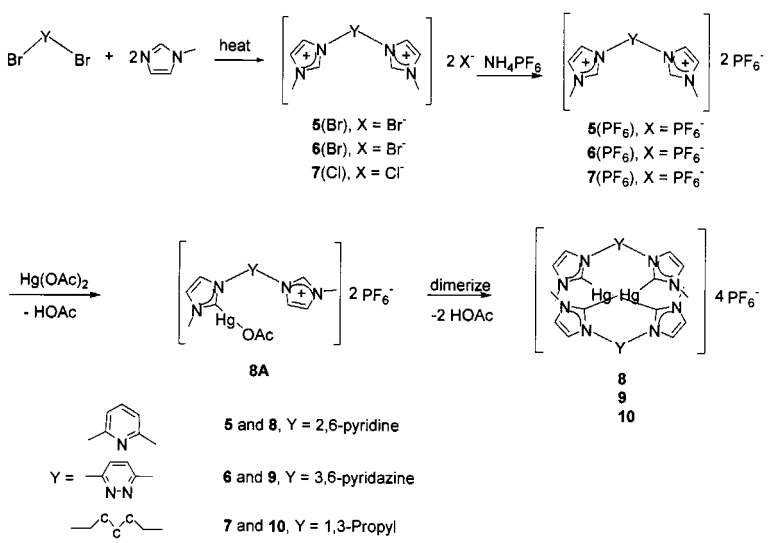

Scheme 2. Synthesis of the ligand precursors, intermediates and double carbene complexes.

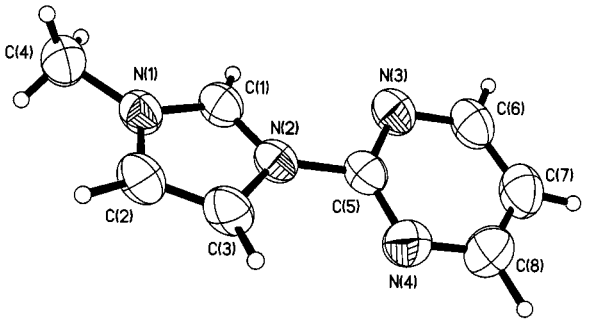

Fig. 1. The ORTEP drawing of **1**(PF_6) (50% thermal ellipsoid). PF_6^- anion is omitted for clarity. Selected bond lengths (Å) and angles (°): C(1)–N(1) 1.315(2), C(1)–N(2) 1.333(2), N(1)–C(2) 1.372(3), N(2)–C(3) 1.381(2), C(2)–C(3) 1.331(3); N(1)–C(1)–N(2) 108.3(2), C(1)–N(1)–C(2) 108.7(2), C(1)–N(2)–C(3) 108.5(2).

respectively. These values are substantially shifted from the chemical shift of 8.34 ppm observed for 1,3-dimethylimidazolium hexafluorophosphate [Meimy-MeH][PF_6]. The increasing acidity of H2 is important to the synthesis of mercury carbene complexes. Therefore while [MeimyMeH][PF_6] does not react with $Hg(OAc)_2$, ligand precursors, **1**(PF_6) and **2**(PF_6) react with $Hg(OAc)_2$ in refluxing acetonitrile to give mercury carbene complexes [Hg (Meimy-pymd)$_2$][PF_6]$_2$ (**3**) and [Hg (py-imy-py)$_2$][PF_6]$_2$ (**4**), respectively.

The crystal structure of **3** (Fig. 2(a)) shows that the mercury ion bonds to two monodentate Meimy-pymd ligands through the carbene carbon atom C(1) and that the linear coordination around the mercury atom deviates from linearity by $\sim 8°$. The important bond angles and distances are listed in the figure caption. The distances of Hg(1)–C(1) and Hg(1)–C(9) are 2.22(3) and 1.97(2) Å, respectively. A weak van der Waals contact of 2.662(2) Å between the nitrogen atom of pyrimidine and Hg atom is observed. This value is within the sum of the van der Waals radii of nitrogen and mercury (3.0 Å) and is shorter than the weak intramolecular Hg–N distance observed in $Hg(C_6H_4CH_2NMe_2\text{-}o)_2$ (2.89(1) Å) [35]. There are also weak interactions between Hg^{2+} and PF_6^-. The distances of Hg(1)···F(6) and Hg(2)···F(12) are 3.04(4) and 3.09(4) Å, respectively and are on the borderline of the sum of van der Waals radii of Hg and F (3.0–3.1 Å) [36]. It appears that deviation from linear coordination around the mercury atom is

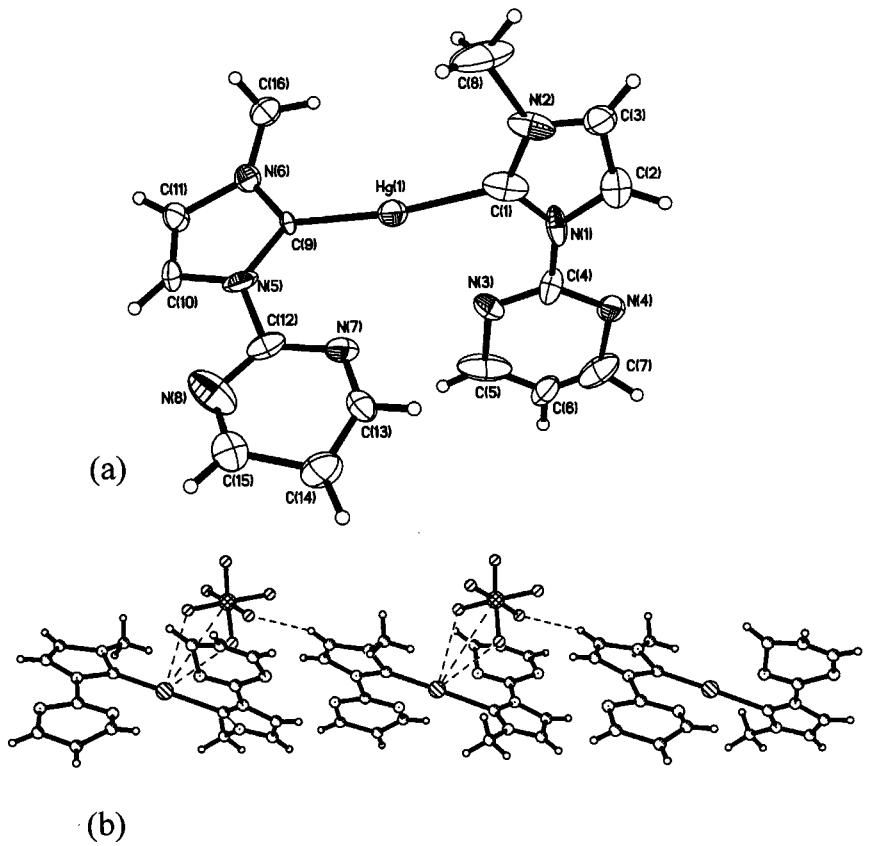

Fig. 2. (a) The ORTEP drawing of **3** (50% thermal ellipsoid). PF_6^- anions are omitted for clarity. Selected bond lengths (Å) and angles (°): Hg(1)–C(1) 2.22(3), Hg(1)–C(9) 1.97(2), C(1)–N(1) 1.22(3), C(1)–N(2) 1.26(3), N(1)–C(2) 1.37(3), N(2)–C(3) 1.24(4), C(2)–C(3) 1.41(3), C(9)–N(5) 1.45(3), C(9)–N(6) 1.42(3), N(5)–C(10) 1.37(3), N(6)–C(11) 1.54(3), C(10)–C(11) 1.20(3); C(1)–Hg(1)–C(9) 172.0(5), N(1)–C(1)–N(2) 108.3(2), C(1)–N(1)–C(2) 108.7(2), C(1)–N(2)–C(3) 108.5(2), N(5)–C(9)–N(6) 100.8(2), C(9)–N(5)–C(10) 131.7(2), C(9)–N(6)–C(11) 102.5(2). (b) Ball and stick representation showing the C–H···F intermolecular contacts of **3**.

caused by these interactions. The PF_6^- anion also forms hydrogen bonds with neighboring cations. The H···F bonds are in the range from 2.24(5) to 2.50(5) Å, within the range of typical hydrogen bonds [35]. The PF_6^- anions thus hold two adjacent cations through Hg···F interactions and H···F hydrogen bonds (Fig. 2(b)). The two *trans* imidazolium ring planes in complex **3** are twisted by an angle of 56.3°. In each monodentate ligand, the pyrimidine ring is almost coplanar with the imidazolium ring (6.8 and 11.2°). The angles are smaller than that observed in the neutral bis(1,3-diphenyl-imidazol-2-ylidene)mercury(II) [29] where the *N*-substituted phenyl rings are rotated by an angle from the imidazolium ring to reduce the steric interactions. Although ligand precursor **2**(PF_6) has two potential *N* coordination sites, in complex **4**, however, the mercury ion selectively binds to the carbene and not to the pyridine nitrogen sites (Fig. 3). The *N*-substituted pyridine rings are almost coplanar with the 2,6-disubstituted imidazolium rings and the two *trans* imidazolium rings are twisted relative to one another by an angle of 59.3°. All the bond angles and bond distances are also comparable to those reported for mercury carbene complexes [27,29].

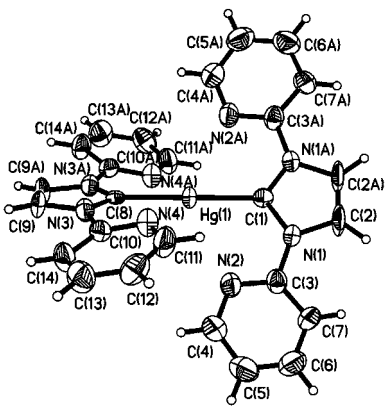

Fig. 3. The ORTEP drawing of **4** (50% thermal ellipsoid). PF_6^- anions are omitted for clarity. Selected bond lengths (Å) and angles (°): Hg(1)–C(1) 2.085(13), Hg(1)–C(8) 2.086(13), C(1)–N(1) 1.350(11), N(1)–C(2) 1.394(13), C(2)–C(2A) 1.27(2), C(8)–N(3) 1.343(11), N(3)–C(9) 1.395(13), C(9)–C(9A) 1.30(2); C(1)–Hg(1)–C(8) 180.00(1), N(1)–C(1)–N(1A) 107.5(12), C(1)–N(1)–C(2) 107.3(9), N(3)–C(8)–N(3A) 108.3(11), C(8)–N(3)–C(9) 107.5(9).

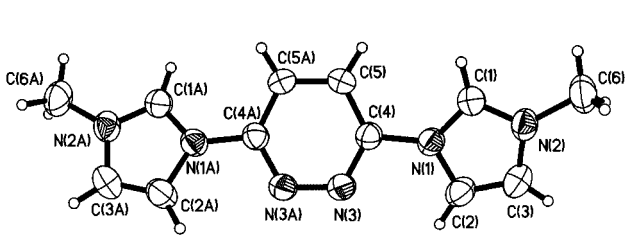

Fig. 4. The ORTEP drawing of **6**(PF_6) (50% thermal ellipsoid). PF_6^- anion is omitted for clarity. Selected bond lengths (Å) and angles (°): C(1)–N(1) 1.338(3), C(1)–N(2) 1.317(3), N(1)–C(2) 1.388(3), N(2)–C(3) 1.370(4), C(2)–C(3) 1.333(4); N(1)–C(1)–N(2) 108.1(2), C(1)–N(1)–C(2) 108.5(2), C(1)–N(2)–C(3) 109.0(2).

2.2. Dinuclear ligand precursors and helical mercury carbene complexes

Ligand precursors **6** and **7** are analogous to **5** which has been reported in our recent preliminary report. These three ligand precursors, after deprotonating the 2-carbene hydrogen, have a topography analogous to tridentate ligands such as 2,6-bis(1-methyl-imidazol-2-yl)pyridine, terpyridine [20–22] and 2,6-dipyrazol pyridine [37], all of which have three potential nitrogen binding sites and have widely been used as tridentate ligands in the formation of supramolecules. Fig. 4 is the crystal structures of **6**(PF_6). All the bond angles and bond distances of the imidazolium rings are comparable to those found in the ligand precursor **1**(PF_6) and those reported in the literatures [34]. The C–H hydrogens of the imidazolium and pyrimidine rings also act as hydrogen bonding donors which form a two dimensional hydrogen bonding network through interactions with PF_6^- anion. The twist angle of imidazolium and pyrimidine rings is 22.3°, which is larger than that in **1**(PF_6) (11.6°).

As was reported in our previous communication, reaction of **5**(PF_6) with mercury acetate produced $[Hg_2(Meimy\text{-}py\text{-}imyMe)_2][PF_6]_4$ (**8**). Similarly, reactions of **6**(PF_6) and **7**(PF_6) with mercury acetate yields dinuclear mercury carbene complexes $[Hg_2(Meimy\text{-}py\text{-}dz\text{-}imyMe)_2][PF_6]_4$ (**9**), and $[Hg_2(pydz\text{-}imyC_3imy\text{-}pydz)_2][PF_6]_2$ (**10**), respectively. The double helical structure of **9** analyzed by X-ray diffraction is given in Fig. 5. Selected bond angles and bond distances are given in the figure captions. All the bond angles and bond distances are comparable to those reported for mercury carbene complexes [27,29]. Note that while the three rings in **5**(PF_6) adopt a banana shape, **6**(PF_6) is a linear shape ligand precursor. Interestingly, despite their difference in geometry, the mercury dicarbene complex **9** also forms a double helical structure rather than other types of structures such as side by side conformer or polymer. In **8**, the helix is formed by bridging two mercury(II) ions with two [Meimy-py-imyMe] strands through the carbene sites. In helicate **9**, the two mercury(II) ions are bridged by two [Meimy-pydz-imyMe] strands through the carbene sites. The coordination around each mercury(II) deviates from linearity by ~8°. This deviation is caused by the weak van der Waals interaction between the PF_6^- anion and mercury ions. One PF_6^- anion bridges further two helical cations through weak interactions with Hg. The two distances of Hg···F are 2.88(4) and 2.95(4) Å and are within the sum of van der Waals radii of Hg and F (3.0–3.1 Å) [36]. The potential binding sites of the deprotonated dicarbene precursor **6**(PF_6) are two carbene carbons as well as two pyrimidine nitrogen atoms. Again, mercury ions only selectively bind to the carbene but not to the pyridazine nitrogen sites. The two imidazolium ring

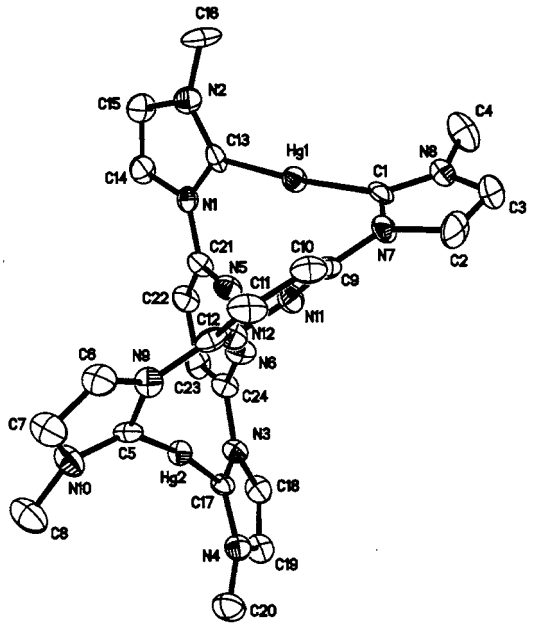

Fig. 5. The ORTEP drawing of **9** (50% thermal ellipsoid). PF_6^- anions and hydrogen atoms are omitted for clarity. Selected bond lengths (Å) and angles (°): Hg(1)–C(1) 2.068(13), Hg(1)–C(13) 2.040(13), Hg(2)–C(5) 2.031(13), Hg(2)–C(17) 2.039(12), C(1)–N(7) 1.338(16), C(1)–N(8) 1.284(15), N(7)–C(2) 1.380(17), N(8)–C(3) 1.383(19), C(2)–C(3) 1.32(2), C(13)–N(1) 1.343(17), C(13)–N(2) 1.356(17), N(1)–C(14) 1.344(16), N(2)–C(15) 1.388(18), C(5)–N(9) 1.391(16), C(5)–N(10) 1.334(16), N(3)–C(17) 1.344(15), N(4)–C(19) 1.361(17)), C(18)–C(19) 1.32(2), C(5)–N(9) 1.343(17), C(5)–N(10) 1.334(16), N(9)–C(6) 1.368(17), N(10)–(C7) 1.388(18);C(1)–Hg(1)–C(13) 174.9(5), N(1)–C(13)–N(2) 105.7(12), C(13)–N(1)–C(14) 109.5(12), C(13)–N(2)–C(15) 109.5(13), N(7)–C(1)–N(8) 107.0(12), C(1)–N(7)–C(2) 109.8(14), C(1)–N(8)–C(3) 110.2(13); C(5)–Hg(2)–C(17) 172.1(5), N(9)–C(5)–N(10) 105.0(11), C(5)–N(9)–C(6) 109.2(12), C(5)–N(10)–C(7) 110.5(12), N(3)–C(17)–N(4) 103.4(11), C(17)–N(3)–C(18) 110.4(11), C(17)–N(4)–C(20) 124.1(12)

planes in the same ligand twist 63.5° to each other. The $Hg^{II}\cdots Hg^{II}$ distance of 6.0(4) Å and the pyridazine N to Hg distance of 2.9(5) Å suggest that there is no $Hg^{II}\cdots Hg^{II}$ interaction and no interaction between pyridazine and mercury. The two *trans* imidazolium ring planes are twisted by an angle of 72.2° to each other. The conformation and the twist angle are comparable to that of $[Ag(pydz\text{-}im_2)_2][PF_6]$ (im = imino nitroxides) [38].

Three possible pathways of helical complex formation are given in Scheme 3. The formation of **8** through pathway I has been discussed briefly in our earlier communication. ^{1}H-NMR spectroscopy has been employed to trace the formation of **8**. Fig. 6(a) and (e), respectively show the ^{1}H-NMR spectrum of the ligand precursor **5**(PF_6) and the helical carbene complex **8**. Fig. 6(b–d), show the spectra taken when an equal molar ratio of **5**(PF_6) was allowed to react with $Hg(OAc)_2$ for 9, 33, and 48 h, respectively at room temperature. From the ^{1}H-NMR spectra of Fig. 6(b–d), the only major species observed other than **5**(PF_6) and **8** is the isolable intermediate $[(OAc)Hg(Meimy\text{-}py\text{-}HimyMe)][PF_6]_2$, **8A**, (a singlet at δ 9.42 for the 2-carbene hydrogen, a doublet-doublet at δ 8.46 and two doublets at δ 7.91 and 7.95 for pyridyl ring protons, four doublets of equal intensity at δ 8.06, 8.19, 7.63 and 7.66 for the imidazole ring protons and two singlet at δ 4.01 and 4.06 for the methyl groups). Solid **8A** was isolated in dimeric form, in which association of two molecular cations through intermolecular hydrogen bonding gives **8B**, which has an approximate double helical topology. Carbene formation through deprotonating of an imidazolium cation in **8B** by a hydrogen bonded acetate, followed by complexation will generate **8D**, which then quickly transforms to the product **8,** again through intramolecular deprotonation and complexation.

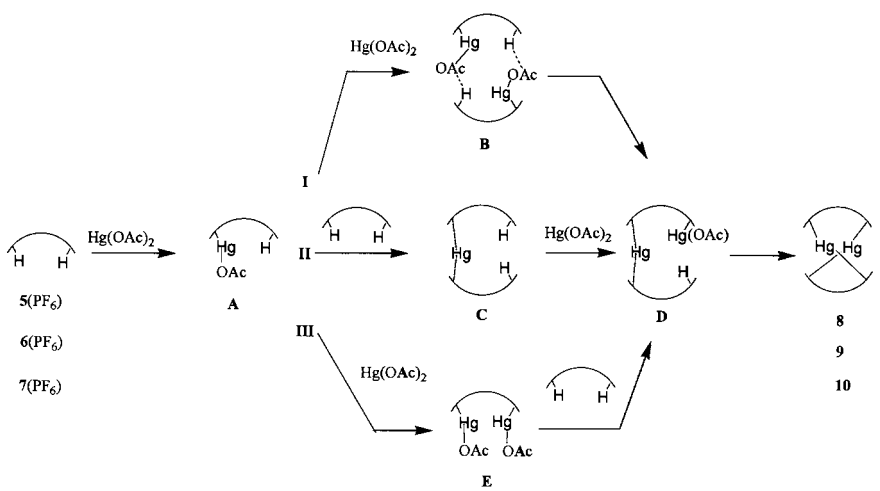

Scheme 3. Three possible pathways (I, II and III) for the format of **8**, **9** and **10** from ligand precursors **5**(PF_6), **6**(PF_6) and **7**(PF_6), respectively, several possible intermediates, **A**, **B**, **C**, **D** and **E** are also shown.

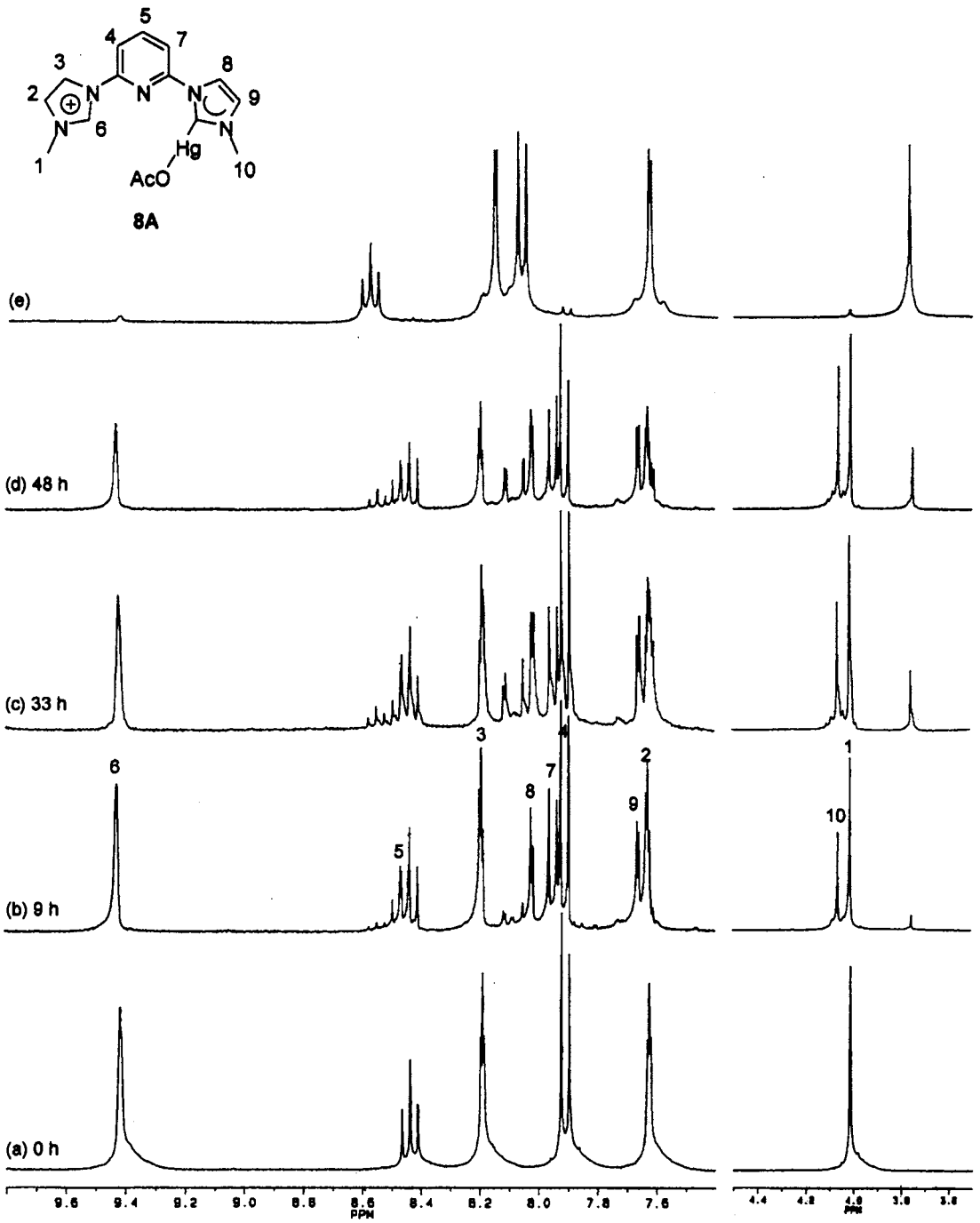

Fig. 6. (a) and (f) are the ^{1}H-NMR spectra of **5**(PF_6) and **8**, respectively. (b), (c) and (d) are the ^{1}H-NMR spectra taken when a mixture (1:1 mol) of **5**(PF_6) and $Hg(OAc)_2$ was allowed to react for 9, 33 and 48 h, respectively at room temperature, in acetonitrile under nitrogen atmosphere. Tentative assignments for intermediate **8A** are given. Only a partial range of each spectrum is given.

We have also followed the reaction pathway of other helical dicarbene complexes by ^{1}H-NMR spectroscopy. Interestingly, the formation of double helical mercury(II) carbene complexes **9** and **10** seems to go through different pathways from that of complex **8**. Fig. 6 shows the ^{1}H-NMR spectra of the reaction of **6**(PF_6) with $Hg(OAc)_2$ in a 1:1 molar ratio as a function of time. When the reaction was allowed to react for 20 min at room temperature, a substantial amount of **9** was formed (Fig. 7(b)). Apparently, the formation of **9** is faster than that of **8** with $Hg(OAc)_2$. Besides a faster reaction rate, the observable intermediates in the formation of **9** are more complicated than that in the formation of **8**. From Fig. 7(b–e) we have been able to identify intermediates **9A**, **9C** and **9E**. Although differentiation of **9A** from **9C** in a spectrum is difficult, this

can be achieved by tracing the relative increment of **9C** versus **9A** with time. The tentative assignments with numberings given in Fig. 6 are **9A**: a singlet at δ 9.48 for the 2-carbene hydrogen, two doublets of equal intensity at δ 8.51 and 8.45 for pyrimidyl ring protons, four doublets of equal intensity at δ 8.14, 7.99, 7.82 and 7.72 for the imidazole ring protons and two singlets at δ 4.19 and 4.11 for the methyl groups; **9C**: a singlet at δ 9.39 for the 2-carbene hydrogen, two doublets of equal intensity at δ 8.52 and 8.46 for pyrimidyl ring protons, four doublets of equal intensity at δ 8.25, 8.18, 7.85 and 7.69 for the imidazole ring protons and two singlets at δ 4.32 and 4.07 for the methyl groups; **9E**: one doublets at δ 8.42 for pyrimidyl ring protons, two doublets of equal intensity at δ 7.87 and 7.73 for the imidazole ring protons and one singlet at δ 4.17 for the methyl groups. It appears that during the early stage of the reaction, deprotonation of the ligand precursor **6**(PF_6) by an acetate, followed by complexation generates [(OAc)Hg(imy-pyrd-Himy)][$(PF_6)_2$] (**9A**), an analogy of **8A**. Intermediate **9A**, can go through pathway I to generate **9**. Alternatively, **9A** can react either with

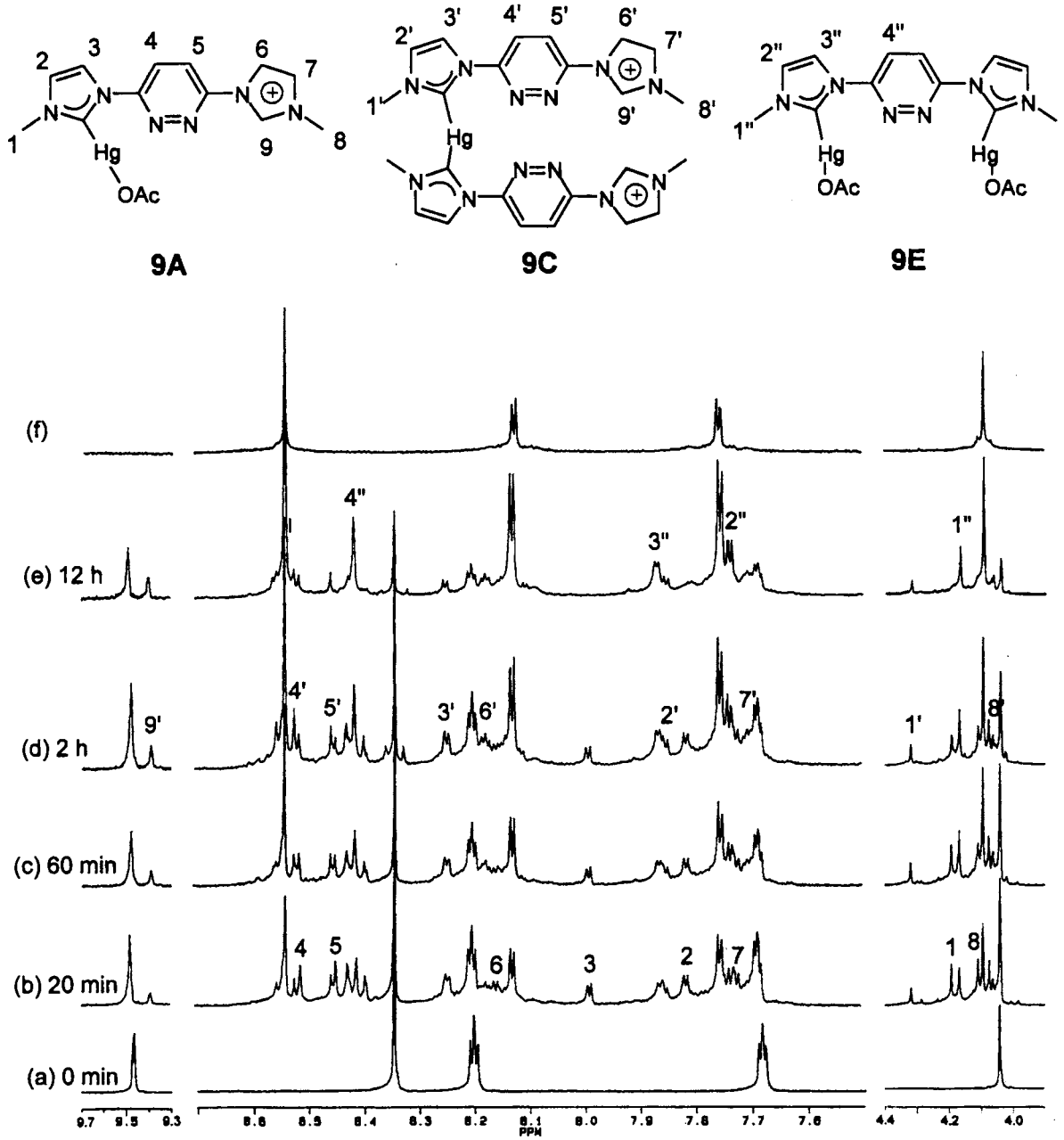

Fig. 7. (a) and (f) are the ^{1}H-NMR spectra of **6**(PF_6) and **9**, respectively. (b), (c), (d) and (e) are the ^{1}H-NMR spectra taken when a mixture (1:1 mol) of **6**(PF_6) and $Hg(OAc)_2$ was allowed to react for 20 min, 1, 2 and 12 h, respectively at room temperature, in acetonitrile under nitrogen atmosphere. Tentative assignments for intermediates **9A**, **9C** and **9E** are given. Only a partial range of each spectrum is given.

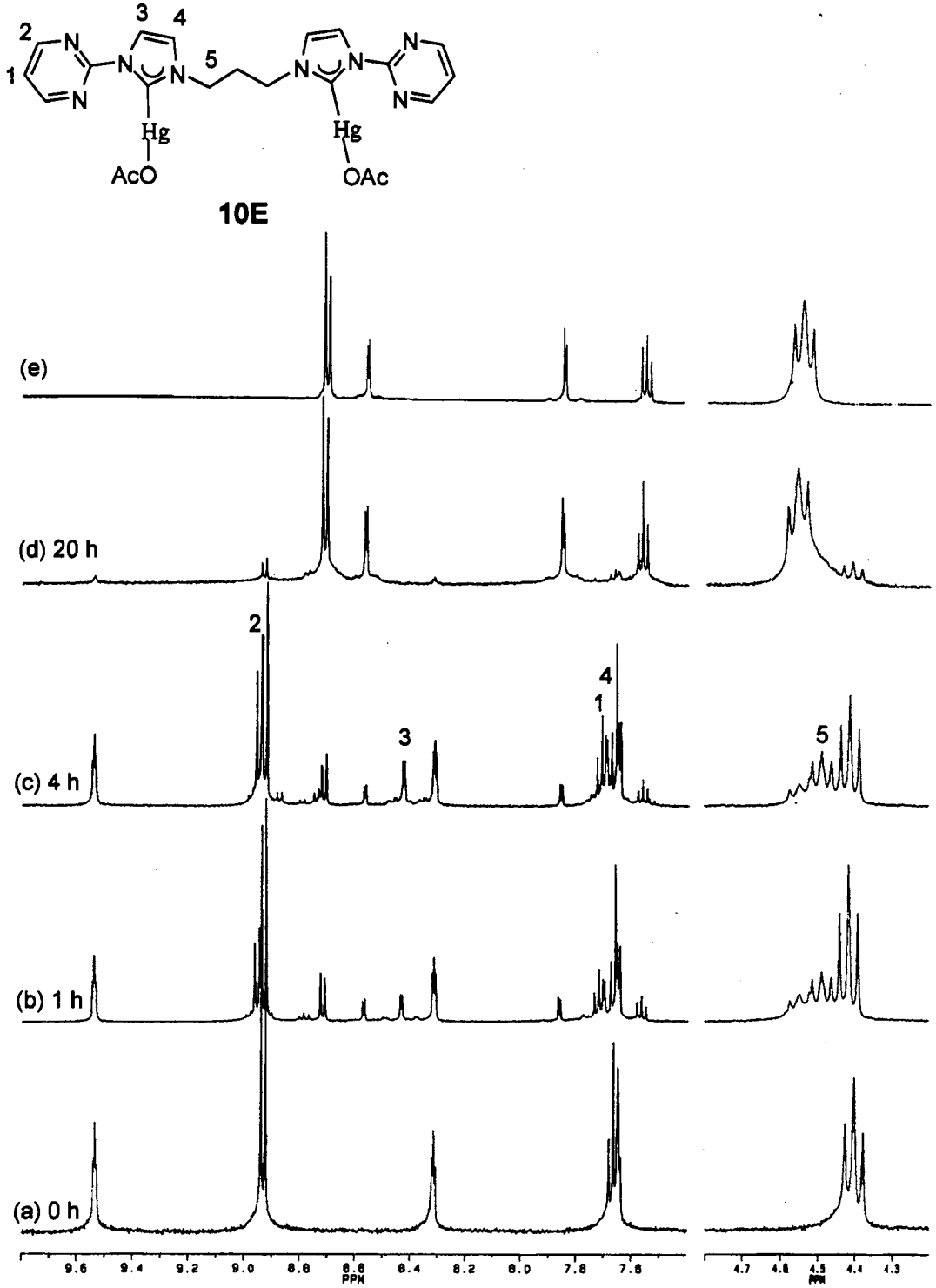

Fig. 8. (a) and (e) are the ^{1}H-NMR spectra of **7**(PF_6) and **10**, respectively. (b), (c) and (d) are the ^{1}H-NMR spectra taken when a mixture (1:1 mol) of **7**(PF_6) and $Hg(OAc)_2$ was allowed to react for 1, 4 and 20 h, respectively at room temperature, in acetonitrile under nitrogen atmosphere. Tentative assignments for intermediate **10E** are given. Only partial range of each spectrum is given.

another free ligand precursor to give intermediate **9C** (Scheme 2, path II) or with $Hg(OAc)_2$ to give intermediate **9E** (Scheme 2, path III). **9C** and **9E** can react, respectively with $Hg(OAc)_2$ and **6**(PF_6) to give the intermediate **9D**, which upon further deprotonation and complexation gives the final double helical mercury carbene complex **9**.

Fig. 8 again is the ^{1}H-NMR spectra for the reaction of **7**(PF_6) complex with $Hg(OAc)_2$ as a function of time. Only an intermediate assignable to **10E** has been ob-

served. This assignment is based on the fact that **10E** has an equivalent methylene groups next to the *N*-heterocyclic carbene nitrogen atom and these is no 2-carbene proton, while the presence of other possible intermediates (**10A** or **10C**) requires nonequivalent methylene groups and in addition, the presence of 2-carbene protons. To further confirm the assignment, a CD_3CN solution with a 1:4 molar ratio of **7**(PF_6) to $Hg(OAc)_2$ in a sealed NMR tube was allowed to heat at 60°C for 16 h, and was then cooled to room temperature. The ^{1}H-NMR spectrum of this sample, reveals the formation of **10E**, which has one doublet at δ 8.92 and a doublet-doublet at 7.73 for the pyrimidyl ring protons, two doublets of equal intensity at δ 8.43 and 7.70 for the imidazole ring protons and two triplets at δ 4.49 and 2.60 for the methylene groups (see Fig. 8 for the assignment with numberings). It is likely that this reaction only goes through pathway III. In this pathway, once the intermediate **10A** being formed, it quickly reacts with another $Hg(OAc)_2$ to give the intermediate **10E**. Further reaction of **10E** with **7**(PF_6) produces the final double helical mercury carbene complexes **10**, probably again via intermediate complex **10D**.

The different formation pathways of the double helical complexes may be caused by two factors. One is the different acidity of the 2-carbene hydrogen, affected by the different spacers or terminal groups. While another reason may be the steric effect around each carbene. In terms of acidity, the chemical shifts of the 2-carbene hydrogens in the ligand precursors **5**(PF_6), **6**(PF_6) and **7**(PF_6) are 9.42, 9.48 and 9.54 ppm, respectively. Ligand precursor **5**(PF_6)**,** having an electron withdrawing pyridine linker, has the least acidic 2-carbene hydrogen. Ligand precursor **6**(PF_6), having a pyridazine linker, has a better electron withdrawing group than that of pyridine, comes next in terms of the acidity of the 2-carbene hydrogen. Ligand precursor **7**(PF_6), having two good electron withdrawing pyrimidines has the most acidic 2-carbene hydrogen among the three. When the less acidic ligand precursor **5**(PF_6) reacts with an equal molar ratio of $Hg(OAc)_2$ to give intermediate **8A**, the 2-carbene hydrogen in the dangling imidazolium ring of **8A** would be blocked by the neighboring coordinated Hg(OAc). This, together with the less acidic property of the 2-carbene hydrogen in **8A**, leads to the formation of an intermolecular hydrogen bonded dimer **8B** rather than to undergo further deprotonation to form **8C** (pathway II) or **8E** (pathway III). Unlike the banana shape of **5**(PF_6), the linear **6**(PF_6) is linear and the 2-carbene hydrogens are more acidic. Once **6**(PF_6) transforms to **9A**, formation of a hydrogen bonded dimer is less sterically favorable. Thus **9A** further reacts with **6**(PF_6) to give intermediate **9C** or reacts with a free $Hg(OAc)_2$ to give the intermediate **9E**. **7**(PF_6) has the most acidic 2-carbene hydrogen and the least rigid linker among the three precursors. **7**(PF_6) may tend to react consecutively with two $Hg(OAc)_2$ to give the major intermediate **10E**. The absence of intermediate **10C** implies that the reaction of **10A** with **7**(PF_6) (pathway II) is much slower than the reaction of **10A** with $Hg(OAc)_2$ (pathway III). It should be emphasized that species which have not been observed in the ^{1}H-NMR spectrum, does not mean that it is not formed. For example, although intermediates **9B**, **10B** have not been observed in the ^{1}H-NMR spectra, however, it is possible that the dimers **9B**, **10B** once formed are transformed to the final products **9** and **10** readily. Likely, intermediates **8D**, **9D** and **10D** have not been detected. This is possibly due to the facile formation of final products from these intermediates. Detail investigations are needed to further confirm the proposed reaction pathways. Note that in those documented reports, when ligands with N, O or S donor atoms are used in the formation of multinuclear helical complexes, isolation of reaction intermediates are not easy. In a recent example reported by Ziessel et al. [39], the formation of copper(I) helicate has been proposed to go through a three-step mechanism, via a $[Cu(L)_2]^{2+}$ intermediate. However, this mononuclear copper intermediate was unable to be isolated or isolated in low yield. Therefore, the relatively slow reaction rate, the variety of topologies and stable intermediates reported in this work allow one to verify the various possible pathways.

In this work, we have prepared several pyridylcarbene ligand precursors of different geometries. Using these ligand precursors, we have succeeded in the synthesis of a series of helical mononuclear and dinuclear mercury carbene complexes. Several mercury(II)–carbene intermediates have been identified and isolated during reactions. Studies suggest that these mercury(II)–carbene double helicates are formed through different mechanisms. Further design of carbene precursors capable of forming extended supramolecules with or without metal ions can be achieved easily. Therefore metal–carbene compounds are very promising for the study of supramolecules. The synthesis of helical carbene complexes with different metal ions is underway. The research grant (NSC 89-2113-M-030-002) from National Science Council of Taiwan is highly appreciated.

3. Experimental

2-Chloropyrimidine was recrystallized in THF before use, while all other chemicals were A.R. grade and were used without further purification. Solvents were dried and freshly distilled under nitrogen prior to use. Elemental analyses were carried out by the Heraeus CHN–O-Rapid Analyzer at the NSF instrumentation Center of Taipei. ^{1}H-NMR measurements were performed on a Bruker AC300 spectrometer at 300 MHz.

All the chemical shifts are quoted in ppm relative to TMS and the coupling constants are in Hz. Signals are expressed as position, multiplicity (s = singlet, d = doublet, t = triplet, m = multiplet), coupling constant, relative integration and assignment.

3.1. X-ray crystal structure determination

Single crystals of **1**(PF_6), **3**, **4** and **6**(PF_6) were obtained from concentrated CH_3CN solutions of the respective complexes, while **9** was obtained from vapor diffusion of diethyl ether into a concentrated EtOH solution. The crystal data of **1**(PF_6), **3**, **4** and **6**(PF_6) were collected on a Siemens P4 diffractometer equipped with a graphite monochromator using a Mo–K_α radiation ($\lambda = 0.71073$ Å). The crystal data of **9** was collected on a Siemens SMART CCD diffractometer equipped with a graphite monochromator using a Mo–K_α radiation ($\lambda = 0.71073$ Å). Details of crystal parameters, data collection and structure refinements are summarized in Table 1. The structures were solved and refined using SHELX 97 [40]. All non-hydrogen atoms, except for some belonging to the solvent molecules, were refined anisotropically. All H atoms, except for water, at calculated positions with thermal parameters equal to 1.2 times that of the attached C atoms were not refined.

3.2. Preparations

3.2.1. Synthesis of 2-(1-methylimidazol-2-yl)pyrimidine chloride, 1(Cl) and hexafluoro-phosphate, 1(PF_6)

A mixture of 2-chloropyrimidine (2.00 g, 26.19 mmol) and 1-methylimidazole (2.15 g, 26.19 mmol) were heated neat at 110°C with stirring for 20 h. The crude product was then recrystallized from MeOH–THF to give a pale yellow product (3.71 g, 72%). ^{1}H-NMR (DMSO-d_6): $\delta = 10.17$ (s, 1H, CH), 9.04 (d, $^3J = 5$ Hz, 2H, CH), 8.44 (dd, $^3J = 2$, $^4J = 1$ Hz, 1H, CH), 7.98 (dd, $^3J = 2$, $^4J = 1$ Hz, 1H, CH), 7.76 (t, $^3J = 5$ Hz, 1H, CH), 4.00 (s, 3H, CH_3); Anal. Calc. for $C_8H_{11}N_4OCl$: C, 44.76; H, 5.17; N, 26.10; Found: C, 44.07; H, 5.12; N, 26.38%. Conversion of the chloride salt to hexafluorophosphate: an aqueous solution (10 ml) of chloride salt (1.47 g, 7.48 mmol) was added to an aqueous solution (10 ml) of the NH_4PF_6 (1.22 g, 7.48 mmol), and was stirred at room temperature (r.t.) for 1 h. The white powder formed was filtered, dried in air, then recrystallized from CH_3CN, the yield was 2.11 g, 92%. ^{1}H-NMR (CD_3CN): $\delta = 9.45$ (s, 1H, CH), 8.91 (d, $^3J = 5$ Hz, 2H, CH), 8.24 (dd, $^3J = 2$, $^4J = 1$ Hz, 1H, CH), 7.63 (t, $^3J = 5$ Hz, 1H, CH), 7.56 (dd, $^3J = 2$, $^4J = 1$ Hz, 1H, CH), 3.99 (s, 3H, CH_3); Anal. calc. for $C_8H_9N_4PF_6$: C, 31.39; H, 2.96; N, 18.30; Found: C, 31.31; H, 2.95; N, 18.20%.

Table 1
Crystal data and structure refinement for **1**(PF_6), **3**, **4**, **6**(PF_6) and **9**

	1(PF_6)	**3**	**4**	**6**(PF_6)	**9**
Empirical formula	$C_8H_9F_6N_4P$	$C_{16}H_{16}F_{12}HgN_8P_2$	$C_{26}H_{20}F_{12}HgN_8P_2$	$C_{12}H_{14}F_{12}N_4P_2$	$C_{24}H_{24}F_{24}Hg_2N_{12}P_4$
Formula weight	306.16	810.90	935.03	504.21	1461.61
Crystal system	Triclinic	Monoclinic	Orthorhombic	Monoclinic	Triclinic
Space group	$P\bar{1}$	Cc	$Pbcn$	$C2/c$	$P\bar{1}$
Unit cell dimensions	$0.3 \times 0.4 \times 0.5$	$0.1 \times 0.4 \times 0.4$	$0.4 \times 0.4 \times 0.5$	$0.3 \times 0.4 \times 0.5$	$0.2 \times 0.2 \times 0.4$
a (Å)	5.8790(10)	13.5632(19)	11.072(2)	15.2259(8)	15.0431(11)
b (Å)	7.9200(10)	9.4138(14)	20.693(3)	10.0167(11)	16.2385(12)
c (Å)	13.5230(10)	19.424(2)	13.225(3)	14.2735(12)	20.0750(14)
α (°)	101.650(10)	90	90	90	109.4870(10)
β (°)	100.620(10)	92.002(12)	90	111.864(6)	97.3720(10)
γ (°)	99.700(10)	90	90	90	107.5190(10)
V (Å^3)	592.12(13)	2478.6(6)	3030.0(10)	2020.3(3)	4263.5(5)
D_{calc} (mg m^{-3})	1.717	2.173	2.050	1.658	2.277
Z	2	4	4	4	4
F(000)	308	1544	1800	1008	2752
Crystal size (mm)	$0.3 \times 0.5 \times 0.4$	$0.1 \times 0.4 \times 0.4$	$0.4 \times 0.5 \times 0.4$	$0.3 \times 0.5 \times 0.4$	$0.5 \times 0.3 \times 0.2$
μ(Mo–K_α) (Å)	0.71073	0.71073	0.71073	0.71073	0.71073
Temperature (K)	293(2)	293(2)	293(2)	293(2)	293(2)
Reflections collected	4132	4083	2469	2873	42180
Independent reflections	2068	3918	2469	2314	18835
Data/restraints/parameters	2068/0/263	3918/2/352	2464/0/224	2314/0/228	18835/0/982
Goodness-of-fit on F^2	1.058	1.096	1.059	1.066	1.240
R_1, wR_2 [$I > 2\sigma(I)$]	0.0345, 0.0898	0.0425, 0.1155	0.0503, 0.1184	0.0579, 0.1526	0.0662, 0.1446
R_1, wR_2 (all data)	0.0383, 0.0928	0.0456, 0.1190	0.0717, 0.1374	0.0705, 0.1626	0.1277, 0.1561
Largest difference peak and hole (e Å^{-3})	0.325, −0.220	1.747, −1.001	2.056, −3.043	0.355, −0.369	2.406, −1.904

*3.2.2. Synthesis of 1,3-bis(pyridyl)imidazolium chloride monohydrate, **2**(Cl)·H_2O and hexafluorophosphate monohydrate, **2**(PF_6)·H_2O*

A mixture of 2-chloropyridine (4.00 g, 35.2 mmol) and 1-methylimidazole (1.45 g, 17.6 mmol) were heated neat at 190°C with stirring for 20 h. The crude product was then recrystallized from MeOH–acetone (1:1) to give a white product (2.92 g, 60%). ^{1}H-NMR ($CDCl_3$): $\delta = 13.01$ (s, 1H; imH), 9.33 (d, 2H; imH), 8.56 (dd, ^3J(H,H) = 4 Hz, 2H; pyH), 8.49 (d, ^3J(H,H) = 2 Hz, 2H; pyH), 8.15 (dt, ^3J(H,H) = 8 Hz, 2H; imH), 7.49 (dd, ^3J(H,H) = 8 Hz, 2H; imH); Anal. Calc. for $C_{13}H_{11}N_4Cl·H_2O$: C, 56.51; H, 4.75; N, 20.29; Found: C, 55.78; H, 4.83; N, 20.13%. Conversion of the chloride salt to hexafluorophosphate salt: An aqueous solution (10 ml) of chloride salt (3.46 g, 12.5 mmol) was added to an aqueous solution (20 ml) of NH_4PF_6 (2.45 g, 15 mmol), and was stirred at r.t. for 0.5 h. The white powder formed was filtered, dried in air, then recrystallized from CH_3CN, the yield was 4.14 g, 90%. ^{1}H-NMR (CD_3CN): $\delta = 10.06$ (s, 1H; imH), 8.67 (d, ^3J(H,H) = 5 Hz, 2H; pyH), 8.33 (s, 2H; imH), 8.17 (dt, ^3J(H,H) = 8, ^4J(H,H) = 2 Hz, 2H; pyH), 7.93 (d, ^3J(H,H) = 8 Hz, 2H; imH), 7.65 (dd, ^3J(H,H) = 8, ^4J(H,H) = 2 Hz, 2H; pyH); Anal. Calc. for $C_{13}H_{11}N_4PF_6$: C, 42.40; H, 3.01; N, 15.22; Found: C, 41.67; H, 2.90; N,4 15.09%.

*3.2.3. Synthesis of bis[(1-methyl-3-pyrimidyl)imidazoline-2-ylidene] mercury(II) dihexafluorophosphate (**3**)*

An CH_3CN solution (50 ml) of **1**(PF_6) (0.38 g, 1.26 mmol) was added to an CH_3CN solution (50 ml) of $Hg(OAc)_2$ (0.2 g, 0.63 mmol) and was refluxed under N_2 for 20 h. The solution was evaporated to dryness and the residue was washed with water. Recrystallization from CH_3CN produced colorless crystals (0.41 g, 81%). ^{1}H-NMR (CD_3CN): $\delta = 8.80$ (d, $^3J = 5$ Hz, 4H, CH), 8.45 (d, $^3J = 2$ Hz, 2H, CH), 7.68 (d, $^3J = 2$ Hz, 2H, CH), 7.61 (t, $^3J = 5$ Hz, 2H, CH), 4.13 (s, 6H, CH_3); Anal. Calc. for $HgC_{16}H_{16}N_8P_2F_{12}$: C, 23.70; H, 1.99; N, 13.82; Found: C, 23.96; H, 1.83; N, 13.64%.

*3.2.4. Synthesis of bis[1,3-bis(pyridyl)-1-imidazoline-2-ylidene] mercury(II) dihexafluorophosphate (**4**)*

An CH_3CN solution (50 ml) of **1**(PF_6) (0.46 g, 1.26 mmol) was added to an CH_3CN solution (50 ml) of $Hg(OAc)_2$ (0.2 g, 0.63 mmol) and was refluxed under N_2 for 20 h. The solution was evaporated to dryness and the residue was washed with water. Recrystallization from CH_3CN produced colorless crystals (0.44 g, 75%). ^{1}H-NMR (CD_3CN): $\delta = 8.40$ (s, 4H, CH), 8.16 (td, $^3J = 8$, $^4J = 2$ Hz, 4H, CH), 8.03 (d, $^3J = 4$ Hz, 4H, CH), 8.48 (dd, $^3J = 8$, $^4J = 5$ Hz, 4H, CH); Anal. Calc. for $HgC_{26}H_{20}N_8P_2F_{12}$: C, 33.40; H, 2.16; N, 11.98; Found: C, 33.38; H, 2.01; N, 11.97%.

*3.2.5. Synthesis of 3,6-bis(1-methylimidazolium-3-yl)pyridazine dichloride, **6**(Cl) and dihexafluorophosphate, **6**(PF_6)*

A mixture of 3,6-dichloropyridazine (1.257 g, 8.44 mmol) and 1-methylimidazole (1.39 g, 16.93 mmol) were heated neat at 110°C with stirring for 20 h. The crude product was recrystallized from MeOH–THF to give a white product (2.09 g, 71%). ^{1}H-NMR (DMSO-d_6) $\delta = 10.37$ (s, 2H, CH), 8.85 (s, 2H, CH), 8.66 (dd, $^3J = 2$, $^4J = 1$ Hz, 1H, CH), 7.68 (dd, $^3J = 2$, $^4J = 1$ Hz, 1H, CH), 4.04 (s, 6H, CH_3). Anal. Calc. for $C_{12}H_{14}N_6Cl_2·2H_2O$: C, 41.27; H, 5.20; N, 24.07; Found: C, 27.27; H, 2.62; N, 16.27%. Conversion of the **6**(Cl) into **6**(PF_6): an aqueous solution (10 ml) of **6**(Cl) (1.173 g, 3.74 mmol) was added to an aqueous solution (10 ml) of NH_4PF_6 (1.22 g, 7.48 mmol), and was stirred at r.t. for 1 h. The white powder formed was filtered, dried in air, then recrystallized in CH_3CN (1.83 g, 92%). ^{1}H-NMR (CD_3CN): $\delta = 9.48$ (s, 2H; imH), 8.34 (s, 2H; pdzH), 8.20 (dd, ^3J(H,H) = 2, ^4J(H,H) = 1 Hz, 2H; imH), 7.68 (dd, ^3J(H,H) = 2, ^4J(H,H) = 1 Hz, 2H; imH), 4.04 (s, 6H; CH_3); Anal. Calc. for $C_{12}H_{14}N_6P_2F_{12}$: C, 27.08; H, 2.65; N, 15.79; Found: C, 27.24; H, 2.66; N, 15.65%.

*3.2.6. Synthesis of 1,3-bis(1-pyrimidylimidazolium-3-yl)propane dibromide, **7**(Br) and dihexafluorophosphate, **7**(PF_6)*

A mixture of 1,3-dibromopropane (1.70 g, 8.44 mmol) and 1-pyrimidylimidazole (0.25 g, 16.93 mmol) were heated neat at 90°C with stirring for 20 h. The crude product was recrystallized from MeOH–THF to give a white product (2.51 g, 58%). ^{1}H-NMR (DMSO-d_6) $\delta = 10.22$ (s, 2H, CH), 9.07 (d, $^3J = 5$ Hz, 4H, CH), 8.54 (d, $^3J = 1$ Hz, 2H, CH), 8.08 (d, $^3J = 1$ Hz, 2H, CH), 7.79 (t, $^3J = 5$ Hz, 2H, CH), 4.43 (t, $^3J = 6$ Hz, 4H, CH_2), 2.60 (m, 2H, CH_2); Anal. Calc. for $C_{17}H_{18}N_8Br_2·H_2O$: C, 39.86; H, 3.94; N, 21.88; Found: C, 40.26; H, 3.95; N, 22.27%. Conversion of the **7**(Br) into **7**(PF_6): an aqueous solution (10 ml) of **7**(Br) (1.92 g, 3.74 mmol) was added to an aqueous solution (10 ml) of NH_4PF_6 (1.22 g, 7.48 mmol), and was stirred at r.t. for 1 h. The white powder formed was filtered, dried in air, then recrystallized in CH_3CN (2.03 g, 87%). ^{1}H-NMR (CD_3CN) $\delta = 9.54$ (s, 2H, CH), 8.93 (d, $^3J = 7$ Hz, 4H, CH), 8.32 (dd, $^3J = 2$, $^4J = 1$ Hz, 2H, CH), 7.68 (t, $^3J = 7$ Hz, 2H, CH), 7.65 (dd, $^3J = 2$, $^4J = 1$ Hz, 2H, CH), 4.42 (t, $^3J = 7$ Hz, 4H, CH_2), 2.61 (m, $^3J = 7$ Hz, 2H, CH_2). Anal. Calc. for $C_{17}H_{18}N_8P_2F_{12}$: C, 32.71; H, 2.91; N, 17.95. Found: C, 32.44; H, 3.07; N, 17.79%.

*3.2.7. Synthesis of bis[3,6-bis(1-methylimidazolium-3-ylidene)pyridazine] dimercury(II) tetrahexafluorophosphate (**9**)*

An CH_3CN solution (50 ml) of **6**(PF_6) (0.34 g, 0.64 mmol) was added to an CH_3CN solution (50 ml) of

$Hg(OAc)_2$ (0.2 g, 0.63 mmol) and was refluxed under N_2 for 20 h. The solution was evaporated to dryness and the residue was washed with water. Recrystallization from CH_3CN produced colorless crystals (0.35 g, 76%). ^{1}H-NMR (CD_3CN): $\delta = 8.54$ (s, 4H; CH), 8.13 (d, $^3J(H,H) = 2$ Hz, 4H; CH), 7.75 (d, $^3J(H,H) = 2$ Hz, 4H; CH), 4.09 (s, 12H; CH_3); Anal. Calc. for $C_{24}H_{24}N_{12}P_4{\cdot}F_{24}Hg_2$: C, 19.72; H, 1.66; N, 11.50; Found: C, 19.83; H, 1.65; N, 11.25%.

3.2.8. Synthesis of bis[1,3-bis(1-pyrimidylimidazolium-3-ylidene)propane] dimercury(II) tetrahexafluorophosphate (**10**)

An CH_3CN solution (50 ml) of **7** (0.40 g, 0.64 mmol) was added to an CH_3CN solution (50 ml) of $Hg(OAc)_2$ (0.2 g, 0.63 mmol) and was refluxed under N_2 for 20 h. The solution was evaporated to dryness and the residue was washed with water. Recrystallization from CH_3CN produced colorless crystals (0.75 g, 71%). ^{1}H-NMR (CD_3CN) $\delta = 8.72$ (d, $^3J = 5$ Hz, 8H, CH), 8.57 (d, $^3J = 2$ Hz, 4H, CH), 7.86 (d, $^3J = 2$ Hz, 4H, CH), 7.56 (t, $^3J = 5$ Hz, 4H, CH), 4.45 (t, $^3J = 8$ Hz, 8H, CH_2), 2.74 (m, 4H, CH_2). Anal. Calc. for $Hg_2C_{34}H_{32}N_{16}P_4F_{24}$: C, 24.81; H, 1.96; N, 13.62; Found: C, 24.79; H, 1.92; N, 13.29%.

4. Supplementary data

Crystallographic data for the structural analysis have been deposited with the Cambridge Crystallographic Data Center, CCDC 147 030–147 034 for **1**(PF_6), **3**, **4**, **6**(PF_6) and **9**. Copies of this information may be obtained free of charge from: The Director, CCDC, 12 Union Road, Cambridge, CB2 1EZ, UK (fax: +44-1223-336033; e-mail: deposit@ccdc.cam.ac.uk or www: http://www.ccdc.cam.ac.uk).

References

[1] D. Bourissou, O. Guerret, F.P. Gabbaï, G. Bertrand, Chem. Rev. 100 (2000) 39.
[2] F.J. Brown, in: S.J. Lippard (Ed.), Progress in Inorganic Chemistry, Wiley, Chichester, 1995, pp. 1–122.
[3] W.A. Herrmann, C. Köcher, Angew. Chem. Int. Ed. Engl. 36 (1997) 2162.
[4] W.A. Herrmann, C. Köcher, L.J. Gooben, G.R.J. Artus, Chem. Eur. J. 2 (1996) 1627.
[5] W.A. Herrmann, M. Elisin, J. Fischer, C. Köcher, G.R.J. Artus, Chem. Eur. J. 2 (1996) 772.
[6] M.F. Lappert, J. Organomet. Chem. 100 (1975) 139.
[7] W.A. Herrmann, L.J. Goosen, C. Kocher, G.R.J. Artus, Angew. Chem. Int. Ed. Engl. 35 (1996) 2805.
[8] W.A. Herrmann, G.M. Lobmaier, M. Elison, J. Organomet. Chem. 520 (1996) 231.
[9] W.A. Herrmann, F.C. Munck, G.R.J. Artus, O. Runte, R. Anwander, Organometallics 16 (1997) 682.
[10] W.A. Herrmann, J. Fischer, K. Öfele, G.R.J. Artus, J. Organomet. Chem. 530 (1997) 259.
[11] W.A. Herrmann, G. Gerstberger, M. Spiegler, Organometallics 16 (1997) 2209.
[12] K. Öfele, W.A. Herrmann, D. Mihalios, M. Elison, E. Herdtweck, T. Priermeier, P. Kiprof, J. Organomet. Chem. 498 (1995) 1.
[13] D. Enders, H. Gielen, G. Raabe, J. Runsink, J.H. Teles, Chem. Ber. 129 (1996) 1483.
[14] D. Enders, H. Gielen, J. Runsink, K. Breuer, S. Brode, K. Boehn, Eur. J. Inorg. Chem. (1998) 913.
[15] D. Enders, H. Gielen, K. Breuer, Tetrahedron: Asymmetry 8 (1997) 3571.
[16] D. Enders, H. Gielen, G. Raabe, J. Runsink, J.H. Teles, Chem. Ber. 130 (1997) 1253.
[17] J.D. Watson, F.H.C. Crick, Nature (London) 171 (1953) 737.
[18] W. Saenger, Principles of Nucleic Acid Structure, Springer, New York, 1984.
[19] U. Koert, M.M. Harding, J.-M. Lehn, Nature (London) 346 (1990) 339.
[20] Lehn, Supramolecular Chemistry — Concepts and Perspectives, VCH, Weinheim, 1995.
[21] F. Vögtle, Supramolecular Chemistry, Wiley, Chichester, 1991.
[22] C. Piguet, G. Bernardinelli, G. Hopfgartner, Chem. Rev. 97 (1997) 2005.
[23] K.M. Lee, C.K. Lee, I.J.B. Lin, Angew. Chem. Int. Ed. Engl. 17 (1997) 1850.
[24] H.M.J. Wang, I.J.B. Lin, Organometallics 17 (1998) 972.
[25] H.M.J. Wang, C.Y.L. Chen, I.J.B. Lin, Organometallics 18 (1999) 1216.
[26] C.K. Lee, J.C.C. Chen, K.M. Lee, C.W. Liu, I.J.B. Lin, Chem. Mater. 11 (1999) 1237.
[27] H.W. Wanzlick, H.J. Schönherr, Chem. Ber. 103 (1970) 1037.
[28] H.W. Wanzlick, H.J. Schönherr, Angew. Chem. Int. Ed. Engl. 7 (1968) 141.
[29] V.P. Luger, G. Ruban, Acta Crystallogr. Sect. B 27 (1971) 2276.
[30] A.J. Arduengo, III, R.L. Harlow, W.J. Marshall, T.K. Prakasha, Heteroat. Chem. 7 (1996) 421.
[31] B. Bildstein, M. Malaun, H. Kopacka, K.H. Ongania, K. Wurst, J. Organomet. Chem. 552 (1998) 45.
[32] B. Bildstein, M. Malaun, H. Kopacka, K.H. Ongania, K. Wurst, J. Organomet. Chem. 572 (1999) 177.
[33] J.C.C. Chen, I.J.B. Lin, J. Chem. Soc. Dalton Trans. (2000) 839.
[34] J. Fuller, R.T. Carlin, H.C. De Long, D. Haworth, J. Chem. Soc. Chem. Commun. (1994) 299.
[35] J.L. Atwood, D.E. Berry, S.R. Stobart, M.J. Zaworotko, Inorg. Chem. 22 (1983) 3480.
[36] J.E. Huheey, E.A. Keiter, R.L. Keiter, Inorganic Chemistry: Principles of Structure and Reactivity, Fourth ed., Harpercollins College Publishers, New York, 1993.
[37] N.K. Solanki, A.E.H. Wheatley, S. Radojevic, M. McPartlin, M.A. Halcrow, J. Chem. Soc. Dalton Trans. (1999) 521.
[38] H. Oshio, T. Yaginuma, T. Ito, Inorg. Chem. 38 (1999) 2750.
[39] R. Ziessel, A. Harriman, J. Suffert, M.-T. Youinou, A. De Cian, J. Fischer, Angew. Chem. Int. Ed. Engl. 22 (1997) 2509.
[40] G.M. Sheldrick, SHELX 97, Progams for Crystal Structure Analysis (Release 97-2), University of Göttingen, Germany, 1998.